



Originally published as:

Wiese, B., Nützman, G. (2009): Transient Leakage and Infiltration Characteristics during Lake Bank Filtration. - Groundwater, 47, 1, 57-68,

DOI: [10.1111/j.1745-6584.2008.00510.x](https://doi.org/10.1111/j.1745-6584.2008.00510.x)

Transient Leakance and Infiltration Characteristics during Lake Bank Filtration

B. Wiese^{1,2}, G. Nützmänn^{1*}

Abstract

Infiltration capacity of bank filtration systems depends on water extraction and hydraulic resistance of the bed sediments. Lake bed hydraulics may be especially affected by clogging, which is dependent on settlement of fine particles, water quality, water temperature, water level, redox potential and other factors. In the field most of these processes are difficult to quantify and thus, when calculating response to pumping the water flux across the sediment surface is assumed to be linearly dependent on the hydraulic gradient. However, this assumption was not adequate to describe conditions at a bank filtration site located at Lake Tegel, Berlin, Germany. Hence, we first assumed the leakage coefficient (or leakance) is spatially distributed and also temporally variant. Furthermore, observations show that the leakance is considerably higher in shallow than in deeper areas; hence, leakance was assumed to be dependent on the existence and thickness of an unsaturated zone below the lake. The proposed explanation of spatial and temporal variability in leakance involves an hypothesis for redox dependent and reversible biogeochemical clogging. The hypothesis is supported by geochemical observations in surface water and ground water. Four leakance approaches are implemented in the ground water flow code MODFLOW and calibrated by inverse modeling using the parameter estimation software PEST. These concepts are evaluated by examining the fit to the hydraulic heads, to infiltration measurements, transport modeling results, and considering the degrees of freedom due to the number of calibration parameters. The leakage concept based on the assumption of the influence of an unsaturated zone on clogging processes best explains the field data.

Key words: Ground water/surface water interaction, lake, inverse modeling, bank filtration, leakage coefficient, leakance, clogging, redox

*Corresponding author: Leibniz-Institute of Freshwater Ecology and Inland Fisheries, Dept. of Eco-Hydrology, Müggelseedamm 310, D-12587 Berlin, Germany, +49 30 64 181 661; nuetzmann@igb-berlin.de

¹ Leibniz-Institute of Freshwater Ecology and Inland Fisheries, Dept. of Eco-Hydrology, Müggelseedamm 310, D-12587 Berlin, Germany

² now at: KompetenzZentrum Wasser Berlin gGmbH, Ciceronstr. 24, D-10709 Berlin, Germany, bernd.wiese@kompetenz-wasser.de

Introduction

During bank filtration, horizontal or vertical collection wells induce a hydraulic gradient that causes infiltration of surface water into the aquifer. Bank filtration provides effective and cost-efficient pre-treatment of surface water and is used in many parts of the world, mainly for drinking water production (Ray et al. 2003). In Europe, predominantly river bank filtration is used (Doussan et al. 1993, Grischek et al. 2003), but in lowland regions where shallow lakes exist within a river system, bank filtration is also used adjacent to lakes, e. g. in Berlin, Germany (Fritz et al. 2004), and in Finland (Miettinen et al. 1997).

For the quantitative and qualitative management of bank filtration systems, flow velocities and travel times need to be known. In contrast to artificial ground water recharge, where the volumes of infiltrating water can be monitored, the hydraulics of bank filtration are governed by extraction only. Thus, infiltration capacity, which depends on well operation and hydraulic resistance of bed sediments, is a crucial factor. The permeability of river beds is known to be time variable because of the influence of shear stress, bed load transport, fluctuations in discharge and water level, hyporheic flow, and change in wetted perimeter (Huettel et al. 2003). River bed resistance also may be affected by clogging by fine sediment, micro-organisms, and precipitation of iron and manganese, oxy-hydroxides and calcium carbonates as well as gas bubbles (Rinck-Pfeiffer et al. 2000, Wood and Basset 1975). Processes of formation and degradation of the clogging layer in lakes differ from those in rivers. Here, the content of suspended material is lower and bed load transport is negligible (Petticrew et al. 2003). Doppler et al. (2007) observed transient changes in leakance (leakage coefficient) due to temperature differences and fluctuation in surface water levels at a lake bank filtration site in Zürich but exchange coefficients between lakes and ground water generally are not reported to be temporally variable under natural conditions or at bank filtration sites.

The bank filtration system at Lake Tegel, in the northwest portion of Berlin, Germany, is characterized by highly transient well operation whereby head differences between the lake and the adjacent ground water show strong temporal variability. High pumping rates cause the water level in the aquifer to drop below lake bed sediments creating an unsaturated zone of variable thickness beneath the lake. In calculating the ground water response to pumping, normally the infiltration from surface water into the adjacent aquifer is described assuming a linear relationship between the water flux across the sediment surface and the hydraulic gradient, where the proportionality coefficient is the leakage coefficient (leakance) (Bear 1979). In terms of modeling, this should be applied using a head-dependent (Cauchy, third type) boundary condition when there is hydraulic connection between the lake and the aquifer and constant flux (Neumann) boundary conditions when there is an unsaturated zone below the lakebed. For example, this change in boundary type is implemented in the River Package and the Reservoir Package (Fenske et al. 1996) of MODFLOW (Harbaugh et al. 2000). In some cases, however, river infiltration is modeled by applying just a head dependent boundary condition (Rötting et al. 2006). Both approaches generally assume that lakebed properties do not change with time and this is not appropriate at Lake Tegel because of highly variable infiltration dynamics. Previously applied nonlinear approaches that use depth-dependent changes of permeability and temperature effects could not describe the behavior (Bouwer and Rice 1989, Schubert 2002, Lin et al. 2003, Doppler et al. 2007) because these models do not capture the mass transfer fluxes or their spatial distributions.

In this paper the hydraulic conductivity of the lakebed is assumed to change both spatially and temporally. Four different empirical concepts of leakance are considered. A clogging concept that takes into account the extent and thickness of the unsaturated zone as the main factor controlling the leakance is developed.

Site Description

The study site is located at Lake Tegel in the northwest of Berlin, Germany. Waterworks Tegel is Berlin's largest waterworks and pumps 45 million m³ per year from 6 well fields around the lake and 2 on the islands in the lake (Figure 1). Pumping from these wells affects hydraulic heads within an area of 50 km².

The two upper aquifers in the model domain as well as Lake Tegel itself were formed during the Quaternary Saale ice-age. Lake Tegel has a maximum depth of 14 m; the deeper regions are filled with thick limnic sediments, which decrease in thickness and pinch out towards the banks (Pachur and Haberland 1977). The water level is controlled and, on average, is 31.3 m asl in the hydrologic summer (May to October) and 31.5 m asl in the hydrologic winter (November to April).

The upper aquifer (1st aquifer) consists of glaciofluvial fine to coarse sand and has a thickness of about 15 m, about half of which is saturated, with a hydraulic conductivity of $3.5 \times 10^{-4} \text{ m s}^{-1}$. The main aquifer (2nd aquifer) also consists of glaciofluvial fine to coarse sand and is between 25 m and 50 m thick and has a hydraulic conductivity between $2 \times 10^{-4} \text{ m s}^{-1}$ below lake Tegel and $5.5 \times 10^{-4} \text{ m s}^{-1}$ near observation well TEG051 (Figure 1). Hydraulic conductivities were obtained from a hydrogeological structural model developed by the company FUGRO (unpublished work, 2000). The 2nd aquifer is predominantly overlain by a glacial till of about 4 m thick, which acts as an aquitard. Well Field West is the main pumping field. The vertical collection wells are screened in the second aquifer, below the aquitard. The 1st and the 2nd aquifers are hydraulically well connected due to holes in the aquitard. The horizontal collection well at Scharfenberg is screened in the 1st aquifer. Exchange with lower aquifers is inhibited by thick Pleistocene mud and silt layers (Pachur and Haberland 1977).

Infiltration Measurements

In situ infiltration measurements were carried out to estimate the leakance at eight locations into the lakebed of Lake Tegel. From infiltration rate Q , leakance L can be calculated as

$$L = \frac{Q}{\Delta h_w A}, \quad (1)$$

where $Q [\text{m}^3 \text{s}^{-1}]$ is the rate of infiltration, $\Delta h_w [\text{m}]$ the difference between the surface water level and the ground water head, $A [\text{m}^2]$ is the area through which the leakage occurs.

In order to obtain Q , infiltration was measured in the field using a seepage meter (Lee 1977, Cherkauer and McBride 1988). The time required for the bag to empty ranged from 20 minutes to 3 hours. Measured ground water levels show that an unsaturated zone exists below all measurement locations, such that $\Delta h_w = \Delta h_{w,u}$ (Figure 3). Under these conditions, water leaves the seepage meter and infiltrates into the subsurface. Infiltration was measured in water depths between 43 cm and 350 cm at 8 locations. Shaw et al. (1990) found it is not necessary to sample more than 10 locations to account for spatial heterogeneity, Cable et al. (2006) used 12 locations. Kaleris (1998) found a poor repeatability of seepage measurements, in contrast Shaw et al. (1990) found 2 measurements adequate. We usually carried out at least 2 and usually 3 measurements at each site, with a repeat accuracy of $\pm 30\%$.

All measurements were made close to observation well 3311 (Figure 2). Hoffmann and Gunkel (2006) carried out infiltration measurements at 7 locations in Lake Tegel between March 2004 and February 2005 in water depths between 40 and 80 cm, using the method described above.

The absolute accuracy of the method is unknown, but advantages and disadvantages are discussed e.g. in Cable et al. (2006) and Kaleris (1998), among others. In the present case, the devices are operated manually, so they only provide an aggregate value over the measured time period. Bioirrigation is insignificant because relevant organisms have not been found in sandy sediments. Water table variations did not occur during the measurements and wind, waves and currents were low at the lake. Also, a superficial clogging layer above the sandy sediments with changing hydraulic conductivity as reported by Kaleris (1998) does not exist in the investigated area. Spatial heterogeneity is an important issue for seepage measurements (Shaw et al. 1990) owing to heterogeneity in sediment lithology. At the present field site, clogging determines the spatial heterogeneity, since clogging strongly reduces the conductivity of native aquifer sediments.

There are advantages in contrast to other field methods, such as the "Open End Test" (Langguth and Voigt 2004). The diameter of the seepage device is larger, resulting in reduced boundary effects. Even more important is that water infiltrates under natural pressure conditions. This prevents hydraulic changes in the near surface layer. The depth of the layer that hydraulically controls the infiltration is accounted for in calculating the leakance even if it is below the penetration depth of the device. Errors may arise, however, if any connection is not leak-proof and some part of the infiltrated water is not detected. But as a direct technique, seepage meters have the potential to validate indirect methods that involve measuring secondary indicators like hydraulic head difference, chemical tracers or mathematical modeling.

Physico-Chemical Parameters

Oxygen, nitrate and sulphate concentrations are affected by the infiltration dynamics (Massmann et al. 2003, Wiese 2006). Between the bank and the well field, 13 observation wells were sampled during the NASRI project (KWB 2005). Only those observation wells that are continuously sampled and show significantly elevated concentrations of sulphate are discussed in this paper. Sulphate and nitrate were analyzed following DIN EN ISO 10304-1/2, DOC following DIN EN 1484, ^{18}O was analyzed following Meyer et al. (2000). Sulphate isotopes were analyzed following Massmann et al. (2003). Oxygen was measured with an oxygen electrode and temperature with a thermometer, both in a flow-through cell during sampling.

Flow Model

The system was simulated using an areal three-dimensional, transient model. Waterworks Tegel extracts water from the two upper aquifers. The hydraulic head differences between the aquifers are smaller than 20 cm, except in the immediate vicinity of the collection wells. At observation wells TEG363, TEG103 and at the inset location (Figure 2) head differences sometimes are higher. The inset is located at Well Field West (Figure 1). Hydraulic conductivities in the model were between $2.9 \times 10^{-4} \text{ m s}^{-1}$ near the inset and $5.5 \times 10^{-4} \text{ m s}^{-1}$ near TEG051 (Fritz 2002). The unconfined storage coefficient was calibrated to 0.2; the confined storage coefficient was set to 5×10^{-5} . To focus on the infiltration processes at Lake Tegel and avoid a large-scale regional model the size of the model area was reduced through appropriate choice of boundary conditions using results from a steady-state regional ground water flow

model, calibrated for the year 2002 (WASY 2004). From this model boundary conditions were developed either using specified head or specified flow conditions (Wiese 2006).

Lake Tegel is simulated as a head dependent internal boundary. Investigations by Parchur (1987) and Ripl et al. (1987) show that there are thick mud layers below 25 m asl that inhibit infiltration. The boundary of Lake Tegel is assigned where the lake bed is above 25 m asl. In the deeper parts of the lake, no infiltration is simulated (Figure 1). Wells in Well Field West are screened in the second aquifer. Ground water recharge of approx. 120-135 mm y⁻¹, which is 25% of annual rainfall, is applied to the upper layer. The bottom is a no-flow boundary, except for a region around TEG051 where the Pleistocene mud and silt layers do not exist due to a glacial trough (Frey 1975). Data from FUGRO (unpublished 2000) indicate that the size of this area is approximately 0.6 km². Heads in the aquifer below indicate a strong hydraulic connection with the 2nd aquifer causing upward flow, which is modeled with a head dependent boundary condition (bottom water in Figure 1).

The simulation was carried out for the time period January 1, 1998 through April 30, 2005. The first 90 days were simulated as steady state, after which the simulation was transient with weekly time steps. Spatially the model is discretized into 7 layers, with thicknesses ranging between 4 m and 8 m. The first aquifer and the aquitard between the first and second aquifer were simulated by one layer each and the second aquifer by 5 layers. The horizontal cell size is 5 m by 5 m close to the inset and 15 m by 50 m next to the boundary. The model was set up using the graphical user interface PMWinPro7 (WebTech360 2003) and run using MODFLOW2000 (Harbaugh et al. 2000).

Leakance

Figure 3 shows a schematic cross section of the infiltration area. A clogging layer, which can be developed e.g. by fine particle deposits, organic compounds and biofilms within the upper centimeters of the aquifer, controls the infiltration. Usually the thickness, M [m] and the hydraulic conductivity, k_f [m s⁻¹] of the clogging layer are unknown. They can be lumped into the leakance (leakage coefficient), L [s⁻¹]

$$L = \frac{k_f}{M} \quad (2)$$

The Darcy velocity v_f [m s⁻¹] is

$$v_f = L \Delta h_w, \quad (3)$$

where Δh_w is the head difference. Because the clogging layer normally is water saturated and the pressure in the unsaturated zone is less than atmospheric, the head difference when an unsaturated zone is present below the lakebed is the water depth in the lake plus the thickness of the clogging layer M . However, if M is small compared to the depth of water in the lake, as it is usually the case, M can be neglected for calculating the driving head.

The Lake Tegel region is hydrogeologically well explored so that aquifer properties are known. Less well known are rates of infiltration from Lake Tegel and upward fluxes of water from the third aquifer. Because infiltration is controlled by the leakance, only these parameters were calibrated. While one uniform value of leakance is sufficient to describe the

leakage of water from the third aquifer, infiltration from Lake Tegel is more complex and four leakance concepts (Case 1 to Case 4) were developed.

For Case 1 to Case 3, depth dependence of leakance is parameterized with $L_i=f(\text{elevation})$, with i from 1 to 7, each comprising an elevation interval of 1 m between 25 m asl and 32 m asl. Their values are multiplied by a dimensionless temporal function $L_t=f(t)$

$$L(f(z,t)) = L_i \cdot L_t \quad (4)$$

where $L(f(z,t))$ is the leakance in space and time. The formulation of $L_i [s^{-1}]$ is identical for Cases 1 through 3; but the values are calibrated separately for each case. The difference among the three cases is only in the formulation of L_t . The program Pest (Doherty 2005) was used to calibrate simultaneously L_i and L_t . The parameterization of the model is summarized in Table 1, and described in detail below:

- Case 1: Leakance is temporally invariant. Nine parameters are used; 7 to parameterize the leakance by depth, 1 for leakance close to TEG242 and TEG233, $L_t=1$ (Equation 4), 1 leakance from the third aquifer.
- Case 2: Between 1998 and 2005, the leakance follows a linear trend, the slope of which is calibrated. Eleven parameters are used, 7 to parameterize the leakance by depth, 1 for leakance close to TEG242 and TEG233, 2 for L_t (linear trend of leakance), and 1 leakance from the third aquifer.
- Case 3: Between 1998 and 2005, leakance may vary temporally bi-monthly. Fifty-four parameters are used, 7 to parameterize the leakance by depth, one for leakance close to TEG242 and TEG233, 45 for L_t (continuously merged trends over periods of 2 months, Equation 4), and 1 leakance from the third aquifer.

In these three cases, the depth dependence of leakance is a function of elevation.

- Case 4 assumes variability of the leakance is a function of the existence and thickness of an unsaturated zone below the infiltration area:

$$L(f(z,t)) = L_0 \cdot \left(1 + p_1 \cdot h_{\text{usat}}^{p_2}\right) \quad (5)$$

where L_0 is the leakance of the lake bed when there is a saturated zone below, i.e., $h_{\text{usat}}=0$ (see Figure 3 for h_{usat}); h_{usat} is the thickness of the unsaturated zone below the clogging layer; p_1 and p_2 are fitting parameters, respectively. This assumption goes against the standard theory and is not physically based. The effect of the variable thickness of the unsaturated zone beneath the lakebed is represented as a lumped parameter including different, complex and partially unknown mechanisms controlling the infiltration through the clogging layer.

We developed this formulation in order to describe a high leakance in shallow water in combination with temporal variability. Similar to our investigations, Schubert (2002) found most water infiltrating in shallow areas. Other studies support the hypothesis that leakance increases due to a change from anoxic to oxic conditions (Okubo and Matsumoto, 1983; Wood and Basset, 1975; Hoelen et al., 2006). Equation 5 was introduced into the reservoir package of MODFLOW2000. Parameters are provided through an additional input file. Including file handling, two subroutines with 142 lines of code are added. The executable and source code can be obtained by the authors. To

account for the unknown catchment size north of Well Field West, an extra leakance parameter was introduced there. Five parameters were used, 3 from Equation 5, and 1 extra value L_0 for the infiltration area close to TEG242 and TEG233, 1 leakance to the third aquifer.

Parameter Estimation

Each of the four leakance cases was calibrated to hydraulic heads using PEST (Doherty 2005), with weights assigned to compensate for the different information content of each head observation. Observation wells 3301, TEG050, TEG051, TEG339, TEG340, TEG341, TEG350, 6034 were included as head targets in PEST. Near the inset, the spatial density of the piezometers is much higher than in the rest of the model domain and hydraulic heads are very similar (Figure 2). Thus, only observations from piezometer 3301, where the time series is longest, were included in parameter estimation. Observation wells TEG233, TEG242 and TEG243 were not included because the no-flow boundary in the north is only valid for several months. Short term variations from the average would seriously disturb the inversion process.

Hydraulic heads are recorded at different frequency. To avoid a period with dense measurements having a much higher impact on the objective function than a period with scarce measurements, each single measurement was weighted according to the time for which it represents the hydraulic head, usually the measurement interval. Hydrographs of different piezometers have a different range of variation, thus a different standard deviation. As the calibrated model should represent the temporal behavior at all measurement locations equally well, the relative deviation is regarded as residual. Consequently, the residuals have a different magnitude at the different measurement locations. Hence, the single observations of each piezometer are divided by the standard deviation of all observations for a particular piezometer.

For Cases 1 to 3 the leakance is discretized with 7 parameters, each representing a depth interval of the bank. To improve the inversion stability and to obtain a smooth depth distribution, the parameters are constrained by prior information, using the formula:

$$\Phi_{pri} = w \sum_{i=1}^{n-1} |\log(leak_i) - \log(leak_{i+1})| \quad (6)$$

Φ_{pri} forms a part of the objective function with $leak$ as the parameter representing the leakance in a depth interval i , and the weighting factor w chosen such that Φ_{pri} contributes less than 1% to the minimized objective function. The other part of the objective function Φ is commonly formed by the squared weighted residuals of measured and simulated hydraulic heads.

Transport Model

Transport simulations were carried out to show the plausibility of temporally variant leakance owing to changes in the lake bed sediment from chemical clogging mechanisms. Transport simulations were performed within inset of the flow model domain (see left side of Figure 2) using MT3DMS (Zheng and Wang 1999). Temperature [$^{\circ}\text{C}$] and ^{18}O [% vs. SMOW] were modeled for the time period between 2002 and 2005. Concentrations in Lake Tegel were assigned as measured values and concentrations of the eastern transport boundary (Figure 1) were assigned such that the observed concentrations in observation well 3304 were met. Temperature was modeled because for Well 13 (Figure 2) the temperature time series are

longer than for ^{18}O , namely available since 2000. All outer boundaries were set to 10 °C, and Lake Tegel was specified using measured water temperature.

The heat transport model was set up with the following parameters: effective porosity of 0.22, aquifer bulk density of 1820 [kg m^{-3}], aquifer heat capacity of $c_s = 800 [\text{J kg}^{-1} \text{°C}^{-1}]$, water heat capacity of $c_w = 4184 [\text{J k g}^{-1} \text{°C}^{-1}]$ (Häfner et al. 1992). Considering the analogy of heat and solute transport equations (Anderson 2005, Voss and Provost 2002) heat transport parameters can be re-arranged so that a thermal diffusivity of $1.3 \times 10^{-6} [\text{m}^2 \text{s}^{-1}]$ and a retardation coefficient of 1.8 [-] were obtained. The latter becomes an empirical factor for heat exchange between the pore water and the matrix providing for a delayed heat transport. Following Bear (1972) and Hopmans et al. (2002) the effects of thermal dispersion are assumed to be negligible compared to conduction and thus the dispersivity parameter was set to zero. An estimation of the modified thermal Peclet number (Anderson 2005) with a range of simulated flux components showed that this system will be dominated by ground water flow.

Results

Head observations are available for different periods from 25 observation wells for more than 7 years. Additionally, 45 ground water physico-chemical parameters were monitored in 18 observation wells for up to 5 years and 28 surface water parameters for more than 7 years. Only a selected portion of these data are discussed in this paper. The omitted data do not contradict the findings presented here.

Hydraulic Heads

Hydraulic heads are highly variable in the entire model area. At observation well TEG050 heads fluctuate 1.7 m (Figure 4); at the inset heads fluctuate 5 m. The water level of Lake Tegel is regulated to 31.3 m asl between April and September and 31.5 m asl between October and March. The thickness of the unsaturated zone varies between 2m and 7 m.

The comparison of measured and simulated hydrographs of observation well TEG050 shows the general behavior of the system (Figure 4). This observation well is located far enough from the well field where pumps are turning on and off. The variations of hydraulic head are caused by pumping of waterworks Tegel, principally of Well Field West. The minor effect of the southward well fields is represented by the southern boundary condition introduced as measured hydraulic heads.

Visually, the fit of all 4 cases appears acceptable (Figure 4). In Table 2 the values of the objective function Φ for selected observation wells and for the entire model are given. Comparing the objective function for well TEG050, Case 3 is the best fit (Table 2). Cases 2 and 4 are similar; Case 1 is the worst representation of the observed ground water dynamics. All wells that are mainly affected by Well Field West (3301, TEG050, TEG051, TEG340, TEG341, TEG350) show this behavior (Table 2).

A differing order of the objective function values for the modeled cases is detectable at only two observation wells. Observation well 6053 is strongly affected by the horizontal well at Scharfenberg. It shows continuously better fit from Case 1 to Case 4. Well TEG243 is located between Well Field West and Well Field East and also shows an increasingly better fit from Case 1 to Case 3 (Table 2), but Case 4 is significantly better than Case 2. Since values of these observation wells are mainly affected by well fields other than Well Field West, they are

not included in the optimization t , therefore their goodness of fit is an important indicator for judging the performance of the model.

Observation well 3301 is affected by the pumping well turning on and off on a daily basis. Daily observations are included in the model but the time discretization is a week. Hence, the modeled daily fluctuations are smoothed. The minimum value of the objective function Φ is high (46 in Table 2) because the daily variance cannot be explained using a model with a weekly time steps. Though observation well 3301 contributes a large part to the objective function of the entire model (Table 2, first row), this does not indicate a poor fit here. Parameters change only slightly if this well is removed from the objective function. This indicates that the parameterization is physically based (Hill 1998).

Leakance

Complementary to numerical modeling the leakance is calculated from infiltration measurements using Equation 1. Following the results of Hoffmann and Gunkel (2006), the thickness of the clogging layer is assumed to be 10 cm. The leakance values calculated from the field measurements are given in Figure 5. Although only scarce measurements exist in deep water, a water balance reveals that the leakage is low there. Using measured infiltration velocity to calculate infiltration rates [$\text{m}^3 \text{s}^{-1}$] in shallow water ($< 2 \text{ m}$ depth) for the model domain, already slightly more water results than extracted by bank filtration. This deviation may be explained with local heterogeneity or the measurement error of infiltration.

For the numerical simulations in Cases 1 to 3 the leakance is parameterized with 7 zones of infiltration depth and 1 zone of depth independent infiltration in the north (Figure 5). Calibrated values for the latter are $5.3 \times 10^{-7} \text{ s}^{-1}$ (Case 1), $6.5 \times 10^{-7} \text{ s}^{-1}$ (Case 2), $4.8 \times 10^{-7} \text{ s}^{-1}$ (Case 3). The saturated leakance L_0 of Case 4 is $4.1 \times 10^{-8} \text{ s}^{-1}$; parameter p_1 is calibrated to 14.8, and parameter p_2 is calibrated to 0.73.

For Case 1 the leakance is considerably higher in deep than in shallow water, but the situation is reversed for Case 4. Here, the steep increase of the leakance at 27.5 m asl corresponds with the beginning of the unsaturated zone (Equation 5, Figures 3 and 5).

The leakance is temporally constant for Case 1. For Cases 2 and 3, the temporal functions L_t are shown in Figure 6. The temporal behavior of Case 3 coincides quite well with the pumping rate. For Case 4 the leakance varies locally, depending on the extent of the unsaturated zone at each model cell (Equation 5). Therefore, unlike Case 1 to Case 3, a global variation can not be presented in this Figure. The calibrated leakance of water from the third aquifer is only slightly different for all cases, ranging from $2.0 \times 10^{-8} \text{ s}^{-1}$ to $2.3 \times 10^{-8} \text{ s}^{-1}$.

Transport

The results of the transport model are obtained using the hydraulic model of Case 3. The transport simulation produced an excellent fit (Figure 7) without additional calibration, suggesting the hydraulic model represents the system well. The travel time between when water infiltrates and arrives at observation wells 3301 and 3302 is approximately 4 months and approximately 2 months to wells TEG371up and TEG372, and approximately one month to well TEG371op.

Transport modeling was not carried out for Case 4 because the MODFLOW reservoir package does not support transport modeling. The Lake Package (Merritt and Konkow 2000),

which includes all functions of the reservoir package and transport modeling, is not available in the version of Processing Modflow Pro (WebTech360 2003) that we used.

Discussion

Temporal and spatial varying leakance

Infiltration measurements show that the leakance is high in shallow water and suggest that leakance decreases towards deeper water (Figure 5). However, no measurements are available below a water depth of 350 cm (lake elevation of 27.9 m asl). Considering the modeled depth distribution of the leakance for Case 1 to Case 3 (Figure 5), it can be seen that the model results underestimate the leakance in the shallower parts of the lake. Increasing the leakance in shallow depths of the model requires a decrease in larger depths; otherwise, too much water would infiltrate into the aquifer. This means, that the leakance in deep water, where no measurements were carried out, is low.

With high leakage in shallow water and low leakage in deep water, the simulated infiltration rates are hydraulically independent of the ground water table because an unsaturated zone exists below the shallow areas. This causes the modeled hydraulic heads to be too high or model cells go dry. Modifications are necessary to maintain the water balance and thus hydraulic heads of the model. The leakance can be increased in deep water and decreased in shallow water (Case 1) or the leakance itself is transient (Figure 6) and similar in all depths (Figure 5) (Case 2 and Case 3). However, previously reported reasons for transient leakance are not applicable to the present field site. They include: (i) sediment compression (Bouwer and Rice 1989), (ii) temperature variation (Lin et al. 2003, Doppler et al. 2007), (iii) surface water level variations (Huettel et al. 2003, Doppler et al. 2007). Consideration of sediment compression and temperature dependence did not improve model results. Surface water level variations are already included in the model and the magnitude is small (usually 31.3 to 31.5 m asl between summer/winter, minimum 31 m asl in summer 2003). Bed load transport (Petticrew et al. 2003) does not occur in a lake and clogging due to suspended matter (Schubert 2002) is not relevant here because suspended solids are below 10 mg l^{-1} with a mean of 3 mg l^{-1} . This is confirmed by comparing the concentration with the temporal variant leakance obtained from Case 3. The concentrations are uncorrelated to the leakance dynamics ($R^2 < 0.15$), like most other physical, chemical and biological lake water parameters (SENSUT 2005). These are temperature, pH, electrical conductivity, O_2 content, O_2 saturation, total colloids, Secchi Depth, BOD1 (biological oxygen demand within 1 day), BOD5, DOC (dissolved organic carbon), loss on ignition of DOC, organic nitrogen, ammonium, total P, ortophosphate, inorganic carbon, sulphate, chloride, silicon, sodium, calcium, potassium, magnesium, total phytoplankton biovolume, chlorophyll-A, phaeophytin and zooplankton biomass. In contrast, nitrate concentrations in lake water are weakly correlated to the calibrated temporal relative leakance with $R^2 = 0.4$. Since nitrate acts as an electron acceptor, it is plausible that it affects the redox dependent infiltration dynamics and that the correlation of the leakance to the extraction rate of the adjacent well field is based on transient clogging in the infiltration zone.

In contrast to the chemical parameters, the dynamics of temporal variant leakance (Case 3) optically varies almost proportionally with the pumping rates (Figure 6). The dynamics coincide very well, but the correlation coefficient is only $R^2 = 0.42$, because some shifts in time and magnitude exists. From this we conclude that the leakance depends on the pumping rate of the well field.

In Case 4 (Equation 5) the leakance depends on the thickness of the unsaturated zone. The thickness depends on the water table and therefore on the pumping rate. In contrast to Case 1 to Case 3, infiltration strongly decreases by depth, as in situ infiltration measurements indicate (Figure 5). The number of calibration parameters is reduced from 1 (Case 2), 54 (Case 3) to just 5. This reduction of degrees of freedom for calibration is an indication of a higher level of physical representation (Hill 1998). The concept of Case 4 is better transferable than Case 1 to Case 3. Observation wells TEG243 and 6053, were not included in the objective function and calibration; thus, they can be used to test the model.

The better fits here are obtained with Case 3 and Case 4. Observation well 6053 is a better indicator for transferability than TEG243, because it is less affected by Well Field West. Here Case 4 provides the best fit. Despite that the hydraulic heads fit better for Case 3, Case 4 is the best representation of the overall hydraulic situation. Nevertheless, the leakance is dependent on the thickness of the unsaturated zone. This can not be explained only for hydraulic reasons. Therefore we include geochemical observations and propose a concept of reversible anaerobic clogging, described below.

Wells are operated discontinuously on an hourly or daily basis. The short-term head variations cause continuous exchange of atmospheric and soil air. The air exchange is proportional to the area of the water table. When the thickness of the unsaturated zone increases, the air exchange also increases. Additionally, a larger area of the infiltration zone is aerated from below.

Degradation of organic carbon in the unsaturated zone is a continuous sink of oxygen and produces CO₂ (Bourg and Bertain 1993). In the present case, the organic carbon only partly derives from DOC, mainly from sedimentary organic matter (Grünheid et al. 2005). The concentrations of oxygen are a function of the elevation and rise/fall of the water table. We will assume oxygen concentrations in observation wells 3310 and 3311 are indicative of the oxygen content of the unsaturated zone. Concentrations in well 3311, located farther from the shore, are generally lower than in well 3310 (Figure 8). Oxygen concentrations in well 3310 are very low after a period of constantly rising water table, such as in August 2002, January 2003, March 2003, October 2003, and April 2004. Concentrations in well 3311 are high when the water table is very low, such as in November 2002, December 2002, February 2003 and May 2003. The water table variations renew the oxygen which is depleted by DOC degradation. Compared to the surface water, concentrations of nitrate in ground water are significantly reduced between July 2002 and April 2004. In observation well 3311 nitrate concentrations are reduced from the mean value of 8.8 mg l⁻¹ to 1.8 mg l⁻¹. Thus, in deeper regions of the lakebed nitrate reducing conditions prevail. Nitrate concentrations in well 3310 only are reduced before summer 2003, from 6.7 mg l⁻¹ in the lake to 2.4 mg l⁻¹ in ground water. After summer 2003 they are similar to lake concentrations. These significantly reduced nitrate concentrations indicate that previously all oxygen had been depleted within the clogging layer. The oxygen that is present derives from exchange processes with the atmosphere.

It is suggested that unsaturated air flow induces a lateral redox gradient at the lakebed and can lead to re-oxidation of sediments. In deeper regions no re-oxidation is possible because no unsaturated zone exists, and redox values are much lower. The absence of an unsaturated zone causes a rapid decrease in oxidation capacity resulting in sulphate reducing conditions (Okubo and Matsumoto 1979, Wood and Basset 1975). Under anaerobic conditions, especially sulphate-reducing conditions, the hydraulic conductivity decreases (Wood and Basset 1975, Okubo and Matsumoto 1983). This occurs due to the production of expolymeric substances of sulphate reducing bacteria (Hoelen et al. 2006, Wood and Basset 1975, Vandevivere and

Baveye 1992). In contact with oxygen, these substances are re-oxidized within a few hours. Increased sulphate concentrations in late summer 2003 (Figure 9) also indicate re-oxidation of reduced sulphur compounds in the clogging layer or in the aquifer during the drawdown in 2003. Measured sulphate concentrations in observation well 3310 and 3311 correlate to water table fluctuations and to the oxygen and nitrate concentrations. Depending on the ground water table and unsaturated air flow, sulphate concentrations in observation wells 3310 and 3311 are between 10 mg l⁻¹ and 40 mg l⁻¹ higher or lower than in lake Tegel. Specific UV absorption at 254 nm of the DOC is significantly increased during this time, which indicates the DOC and this sulphate derives from reoxidized organic compounds, presumably the same compounds responsible for anaerobic clogging (KWB 2005). Observation well 3301, however, shows reduced sulphate concentrations in summer 2003. Because the deep observation well is closest to the bank, it receives different water. During ground water withdrawal in 2003, infiltration is shifted to deeper areas, and formerly stagnant water is mobilized. Part of this water infiltrated slowly under sulphate reducing conditions, thus showing reduced sulphate concentrations. Increased nitrate concentrations in the surface water increase the oxidation state of the clogging layer and thus probably reduce anaerobic clogging and vice versa. This means that the observed correlation of nitrate to leakance might be physically based.

Consequently, Equation 5 is used to approximate anaerobic clogging and allows us to reduce the number of leakance parameters from 11 (Case 2) or 54 (Case 3) to just 5 (Case 4). This reduction of degrees of freedom for calibration already is an indication of a higher level of physical representation (Hill 1998). The hypothesized anaerobic leakance concept permits a consistent interpretation of hydraulic heads on regional scale, in situ infiltration measurements and geochemical observations. However, measured leakance in shallow water is still higher than simulated values. This indicates that the leakance modeling in Case 4 is a first approximation, because oxygen consumption and unsaturated air flow are represented indirectly by the thickness of the unsaturated zone.

Schubert (2002) detected that infiltration and therefore leakance in shallow water depths of the Rhine River is significantly higher than in deeper areas. He hypothesized clogging of the riverbed with fine particles in deeper areas. His observations could also be explained by anaerobic clogging. Doppler et al. (2007) observed transient leakance that they attributed to temperature dependence and fluctuation of surface water levels, similar to findings of Huettel et al. (2003). Since the surface water level affects the thickness of the unsaturated zone, the reasons for transient leakance might be similar. The present process may be important wherever anaerobic conditions in the clogging layer occur and when an unsaturated zone exists below the surface water body.

Conclusions

The results of this study indicate that:

- The spatial distribution of the leakance (leakage coefficient) is high in shallow water close to the bank and low towards deeper water in the middle of the lake.
- Leakance varies temporally. The magnitude of this temporal variability changes proportionally with the pumping rate of the adjacent well field.
- Leakance increases depending on the thickness of the unsaturated zone. As consequence, a declining water table increases infiltration through the unsaturated zone, although a thick unsaturated zone decouples the water table from the infiltration area.

The hydraulic situation alone can not explain the observed behavior. We explain the variability of the leakance with anaerobic clogging. Under saturated conditions the clogging layer is anaerobic, which enables anaerobic bacteria in the lake bed to produce extra-cellular substances that cause strong clogging. When the ground water level decreases, atmospheric oxygen is transported into the growing unsaturated zone beneath the lake with the result that the anaerobic clogging layer can be oxidized and disintegrates. The process is reversible since oxygen and other electron acceptors continuously are consumed due to the metabolization of organic matter. If the unsaturated zone becomes saturated, the oxygen supply is cut off and anaerobic clogging is re-established.

The consequences for the investigated site and the well operation are:

- The wells are operated discontinuously. This causes fluctuation of the water table followed by an enhanced exchange of soil air with atmospheric oxygen. Therefore, clogging is reduced and infiltration is increased compared to continuous well operation with the same ground water level.
- If it is not possible to incorporate a transient leakance into a ground water management model, the infiltration amounts may be approximately simulated by shifting the maximum leakance to deep water (this refers to case 1).

The modeling approach presented in this paper is one step forward in understanding the complex mechanisms of surface water – ground water interaction during lake bank filtration. Further measurements are needed to explore the relation of the subsurface oxidation state to the leakance and leakage rate, as well as applications to other test sites. Rigorous modeling would require the coupled modeling of ground water flow, unsaturated air flow, and chemical reactions of at least the redox sensitive components oxygen, nitrate and sulphate, and the change in lake bed permeability as a function of redox.

Acknowledgements

This work was carried out in the NASRI project, funded by KompetenzZentrum Wasser Berlin, Veolia Water and Berlin Water Works. The authors are grateful to Anja Hoffmann (Technical University Berlin) and the Berlin municipal authority for providing data of infiltration measurements and physicochemical parameters of Lake Tegel. Tobias Rötting and two anonymous reviewers provided comments that significantly enhanced interpretation of measured data and modeling results. The Editor-in-Chief of the journal edited the paper for English usage and provided helpful technical comments.

References

- Anderson, M. P. 2005. Heat as a ground water tracer. *Ground Water* 43 no. 6: 951-968.
- Bear, J. 1979. *Hydraulics of Groundwater*, McGraw Hill Inc., New York.
- Bourg, A. C., and C. Bertin. 1993. Biogeochemical processes during the infiltration of river water into an alluvial aquifer. *Environmental Science and Technology* 27 no. 4: 661-666.
- Bouwer, H., and R. C. Rice. 1989. Effect of water depth in groundwater recharge basins on infiltration. *Journal of Irrigation and Drainage Engineering* 115 no. 4: 556-567.
- Cable, J. E., Martin, J. B., and Jaeger, J. 2006. Exonerating Bernoulli? On evaluating the

- physical and biological process affecting marine seepage meter measurements. *Limnol. Oceanogr.: Methods* 4: 172-183.
- Cherkauer, D. A., and J. M. McBride. 1988. A remotely operated seepage meter for use in large lakes and rivers. *Ground Water* 26 no. 2: 165-171.
- DIN EN 1484, Water analysis - Guidelines for the determination of total organic carbon (TOC) and dissolved organic carbon (DOC), www.din.com
- DIN EN ISO 10304-1/2, Water quality - Determination of dissolved fluoride, chloride, nitrite, orthophosphate, bromide, nitrate and sulphate ions, using liquid chromatography of ions - Part 1: Method for water with low contamination (ISO 10304-1:1992); Part 2: Determination of bromide, chloride, nitrate, nitrite, orthophosphate and sulphate in waste water (ISO 10304-2:1995), www.din.com
- Doherty, J. 2005. PEST - Model-Independent Parameter Estimation. User Manual 5th Edition, Watermark Numerical computing.
- Doussan, C., A. Toma, B. Paris, G. Poitevin, E. Ledoux, and M. Detay. 1994. Coupled use of thermal and hydraulic head data to characterize river- groundwater exchanges. *Journal of Hydrology* 153 no. 1-4: 215-229.
- Fenske, J. P., S. A. Leake, and D. E. Prudic. 1996. Documentation of a computer program (RES1) to simulate leakage from reservoirs using the modular finite-difference groundwater flow model (MODFLOW), Open-File Report 96-364, U.S. Geological Survey
- Frey, W. 1975. Zum Tertiär und Pleistozän des Berliner Raumes. *Zeitschrift der Deutschen Gesellschaft für Geowissenschaften* 126: 281-292.
- Fritz, B. 2002. Untersuchungen zur Uferfiltration unter verschiedenen wasserwirtschaftlichen, hydrologischen und hydraulischen Bedingungen, Free University Berlin, Berlin, 203 pp..
- Fritz, B., Rinck-Pfeiffer, S, Nützmann, G. and B. Heinzmann. 2004. Conservation of water resources in Berlin, Germany, through different re-use of water. in *Wastewater re-use and groundwater quality*, edited by J. Steenvorden and T. Endreny, pp. 48-53
- Grischek, T., Schönheinz, D., Worch, E., Hiscock, K. 2002. Bank filtration in Europe - An overview of aquifer conditions and hydraulic controls. in *Management of Aquifer Recharge for Sustainability*, edited by P. J. Dillon, Swets & Zeitlinger, Lisse.
- Grünheid, S., G. Amy, and M. Jekel. 2005. Removal of bulk dissolved organic carbon (DOC) and trace organic compounds by bank filtration and artificial recharge. *Water Research* 39 no. 14: 3219-3228.
- Häfner, F., Sames. D. and H.-D. Voigt 1992. Wärme- und Stofftransport. Springer Berlin.
- Hill, M. C. 1998. Methods and guidelines for effective model calibration, U.S. Geological Survey Water-Resources Investigations Report 98-4005.
- Harbaugh, A. W., E. R. Banta, M. C. Hill, and M. G. McDonald. 2000. MODFLOW-2000, The U.S. Geological Survey modular ground-water model. User guide to Modularization concepts and the ground-water flow process., Open-file report 00-92, U.S. Geological

- Survey, Hunter, KS.
- Hoelen, T. P., C. J.A., G. D. Hopkins, C. A. Lebron, and M. Reinhard. 2006. Bioremediation of cis-DCE at a sulfidogenic site by amendment with propionate. *Ground Water Monitoring and Remediation* 26 no. 3: 82-91.
- Hoffmann, A., and G. Gunkel. 2006. Dynamik und Funktionalität des sandigen Interstitials unter dem Einfluss induzierter Uferfiltration. paper presented at DGL, Dresden.
- Hopmans, J. W., J. Simunek, and K. L. Bristow. 2002. Indirect estimation of soil thermal properties and water flux using heat pulse probe measurements: Geometry and dispersion effects. *Water Resources Research* 38 no. 1: 1-14.
- Huettel, M., H. Roy, E. Precht, and S. Ehrenhauss. 2003. Hydrodynamical impact on biogeochemical processes in aquatic sediments. *Hydrobiologia* 494: 231-236.
- Kaleris, V. 1997. Quantifying the exchange rate between groundwater and small streams. *Journal of Hydraulic Research* 36 no. 6: 913-932.
- KWB (2005) Natural and artificial systems of recharge and infiltration, Project database and final Project Report, Kompetenzzentrum Wasser Berlin, unpublished, available on request.
- Langguth, H.-R., and R. Voigt. 2004. Hydrogeologische Methoden, Springer Verlag, Heidelberg.
- Lee, D. R. 1977. A device for measuring seepage flux in lakes and estuaries. *LIMNOL. & OCEANOGR.* 22 no. 1 , Jan.1977: 140-147.
- Lin, C., D. Greenwald, and A. Banin. 2003. Temperature dependence of infiltration rate during large scale water recharge into soils. *Soil Science Society of America Journal* 67 no. 2: 487-493.
- Massmann, G., M. Tichomirowa, C. Merz, and A. Pekdeger. 2003. Sulfide oxidation and sulfate reduction in a shallow groundwater system (Oderbruch Aquifer, Germany). *Journal of Hydrology* 278 no. 1-4: 231-243.
- Merritt, M.L., and L.F. Konikow. 2000. Documentation of a computer program to simulate lake-aquifer interaction using the MODFLOW ground-water flow model and the MOC3D solute-transport model. U.S. Geological Survey Water-Resources Investigations Report 00-4167.
- Meyer, H., L. Schönicke, U. Wand, H. W. Hubberten, and H. Friedrichsen. 2000. Isotope studies of hydrogen and oxygen in a shallow groundwater system (Oderbruch Aquifer, Germany). *Journal of Hydrology* 278: 231-243.
- Miettinen, I. T., T. Vartiainen, and P. J. Martikainen. 1997. Changes in water microbial quality during bank filtration of lake water. *Canadian Journal of Microbiology* 43 no. 12: 1126-1132.
- Okubo, T., and J. Matsumoto. 1979. Effect of infiltration rate on biological clogging and water quality changes during artificial recharge. *Water Resources Research* 15 no. 6: 1536-1542.

- Okubo, T., and J. Matsumoto. 1983. Biological clogging of sand and changes of organic constituents during artificial recharge. *Water Research* 17 no. 7: 813-821.
- Pachur, H. J., and W. Haberland. 1977. Untersuchungen zur morphologischen Entwicklung des Tegeler Sees. *Die Erde* 108 no. 4: 320-341.
- Pachur, H.-J. 1987. die Seen Berlins als Objekte geographischer Forschung -Ergebnisse und Aspekte. paper presented at Verhandlungen des Deutschen Geographentages, Stuttgart.
- Petticrew, E. L., I. G. Droppo, and B. Kronvang. 2003. Interactions between sediments and water. *Hydrobiologica* 494: 1-4.
- Ray, C. 2002. Riverbank filtration: Understanding contaminant biogeochemistry and pathogen removal., 253 pp., Kluwer Academic Publishers, Dordrecht-Boston-London.
- Rinck-Pfeiffer, S. M., S. Ragusa, P. Szajnbok, and T. Vandeveld. 2000. Interrelationships between biological, chemical and physical processes as an analogue to clogging in Aquifer Storage and Recovery (ASR) wells. *Water Research* 34 no. 7: 2110-2118.
- Ripl, W., S. Heller, and C. Linnenweber. 1987. Limnologische Untersuchungen an den Sedimenten des Tegeler Sees, Eigenverlag Fachgebiet Limnologie, Technische Universität Berlin, Berlin.
- Rötting, T. S., J. Carrera, B. J., and S. J.M. 2006. Stream-Stage response tests and their joint interpretation with pumping tests. *Groundwater* 44 no. 3: 371-385.
- Schubert, J. 2002. Hydraulic aspects of riverbank filtration - Field studies. *Journal of Hydrology* 266 no. 3-4: 145-161.
- Shaw, R. D., and E. E. Prepas. 1990. Groundwater-lake interactions: I. Accuracy of seepage meter estimates of lake seepage. *Journal of Hydrology* 119 no. 1-4: 105-120.
- SENSUT. 2005. Physical, chemical and biological data of Lake Tegel, unpublished, available on request from Senatsverwaltung für Gesundheit, Umwelt und Verbraucherschutz, Berlin.
- Vandevivere, P., and P. Baveye. 1992. Saturated hydraulic conductivity reduction caused by aerobic bacteria in sand columns. *Soil Science Society of America Journal* 56 no. 1: 1-13.
- Voss, C.I. and Provost, A.M. 2002. SUTRA, a model for saturated-unsaturated variable density ground-water flow with energy or solute transport: U.S. Geological Survey Open-File Report 02-4231, 250 pp.
- WASY. 2004. Hydrogeologisches Fachgutachten zur Auswirkung grundlegender Änderungen des Betriebs zur Grundwasseranreicherung Wasserwerk Tegel, unveröffentlichter Projektbericht, WASY Gesellschaft für wasserwirtschaftliche Planung und Systemforschung mbH.
- WebTech360. 2003. Processing Modflow Pro - Users Manual, WebTech360, Fairbanks, USA.
- Wiese, B. 2006. Spatially and temporally scaled inverse hydraulic modelling, multi tracer transport modelling and interaction with geochemical processes at a highly transient bank

filtration site, 233 pp, Humboldt-University Berlin, Berlin, <http://edoc.hu-berlin.de/dissertationen/wiese-bernd-ulrich-2006-12-20/PDF/wiese.pdf>.

Wood, W. W., and R. L. Bassett. 1975. Water quality Changes related to the development of anaerobic conditions during artificial recharge. *Water Resources Research* 11 no. 4: 553-558.

Zheng, C., and P. P. Wang. 1999. MT3DMS: A modular three-dimensional multispecies model for simulation of advection, dispersion and chemical reactions of contaminants in groundwater systems, Documentation and User's Guide, U.S. Army Engineer Research and Development Centre, Vicksburg.

Figures

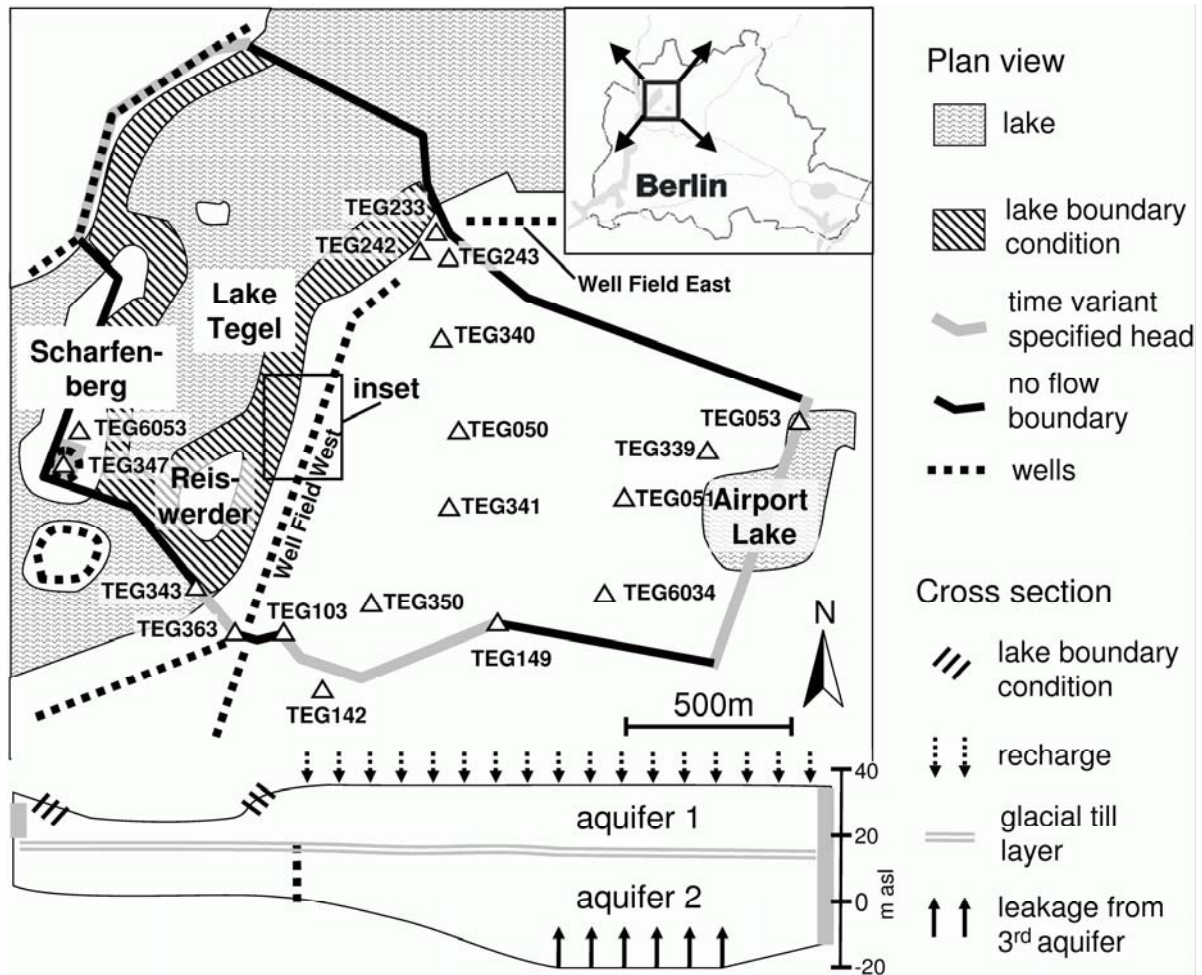


Figure 1: Plan view of the model domain. Lake Tegel is represented as an alternating constant flux/head dependent boundary. Leakage from an underlying (third) aquifer is introduced as a head-dependent boundary condition. A horizontal well is located at the same position as observation well TEG347. It is assigned to aquifer 1 using a time variant specified head boundary. The other time variant specified heads are assigned to both aquifers. Well Field West is assigned to aquifer 2. Gaps in the glacial till are not shown here. The inset is shown in detail in Figure 2.

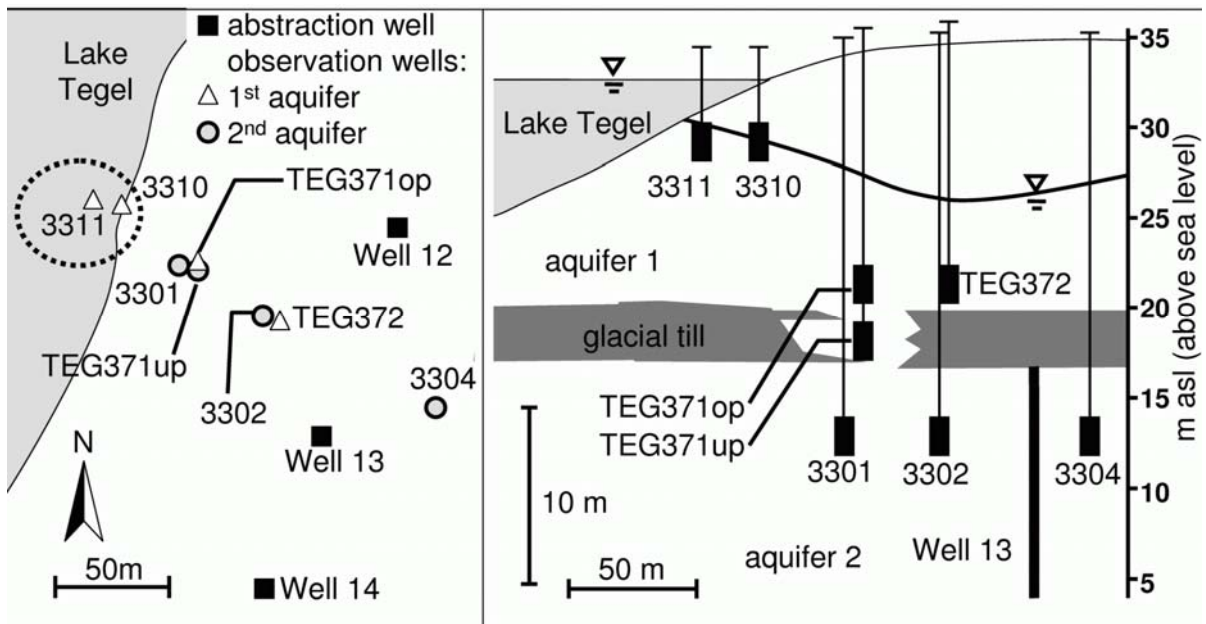


Figure 2: Location of the observation and pumping wells in the inset shown in Figure 1. Triangles represent observation wells screened in the first aquifer. Circles represent observation wells screened in the second aquifer and squares represent pumping wells screened in the second aquifer. The dashed oval indicates where infiltration was measured. A cross section is shown at the right. Black rectangles indicate well screens. Borehole profiles show the gap in the glacial till at well TEG371. Probably other gaps exist.

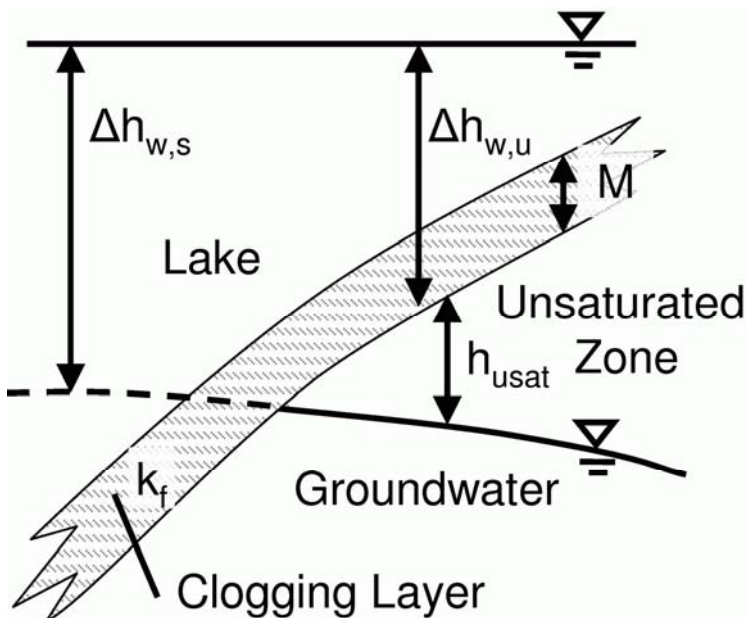


Figure 3: Schematic cross section of the infiltration area shown in Figure 2. The driving head causing infiltration is $\Delta h_{w,s}$ under saturated conditions, and $\Delta h_{w,u}$ when an unsaturated zone exists. M is the thickness and k_f is the hydraulic conductivity of the clogging layer; h_{usat} is the thickness of the unsaturated zone. The solid line represents the water table; the dashed line represents the potentiometric surface.

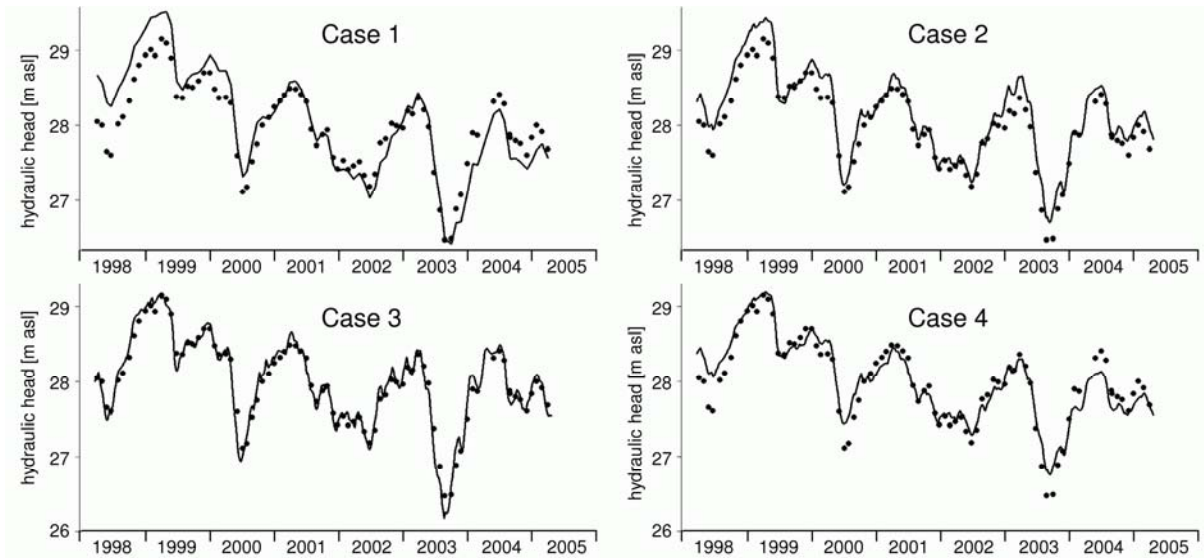


Figure 4: Heads in observation well TEG050. The dots represent the observations; the line represents the simulated heads. The objective function is presented in Table 2.

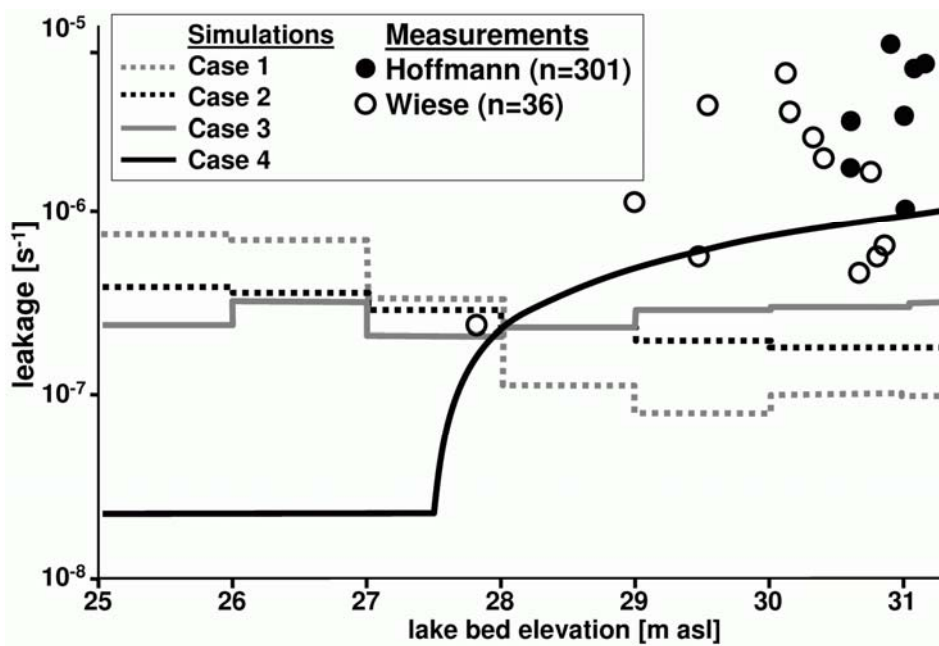


Figure 5: Measured and simulated leakance of the lake bed. Each point represents the mean value at a the measurement location where at least 2 single measurements were made, “n” is the number of measurements. Measurements of Hoffmann and Gunkel (2006) were made between March 2004 and February 2005; measurements for this study (Wiese) were made in June and July

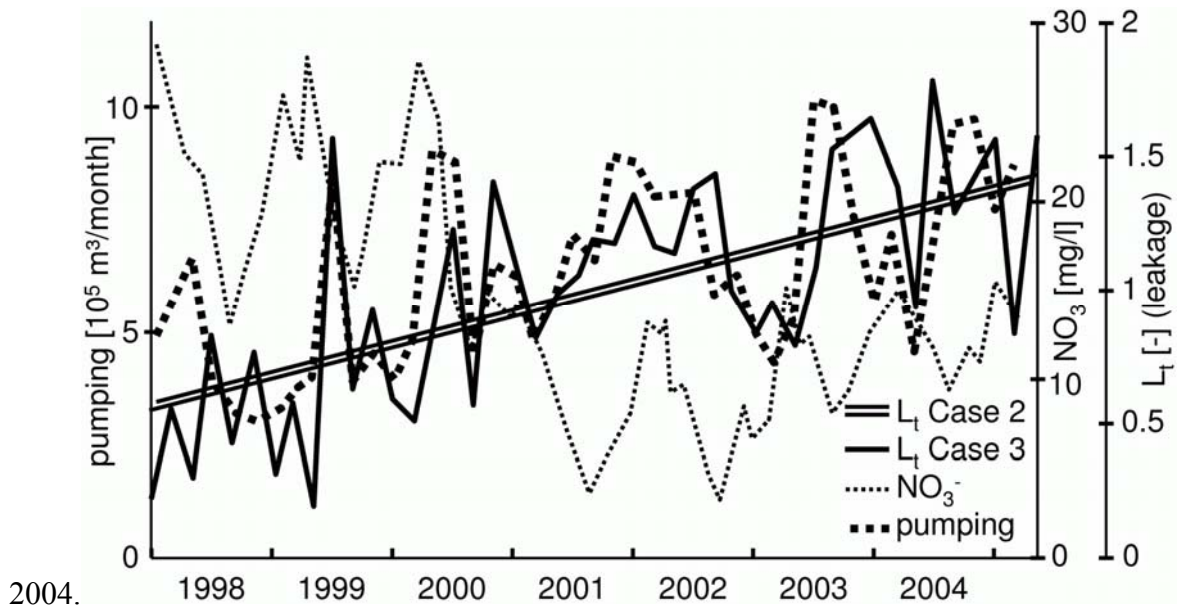


Figure 6: Temporal relative leakance L_t for Case 2 (double straight line) and Case 3 (right axis, straight line). The pumping rate is the monthly average of pumping rate at Well Field West (dashed bold line). Nitrate concentrations are those measured in Lake Tegel (dashed line).

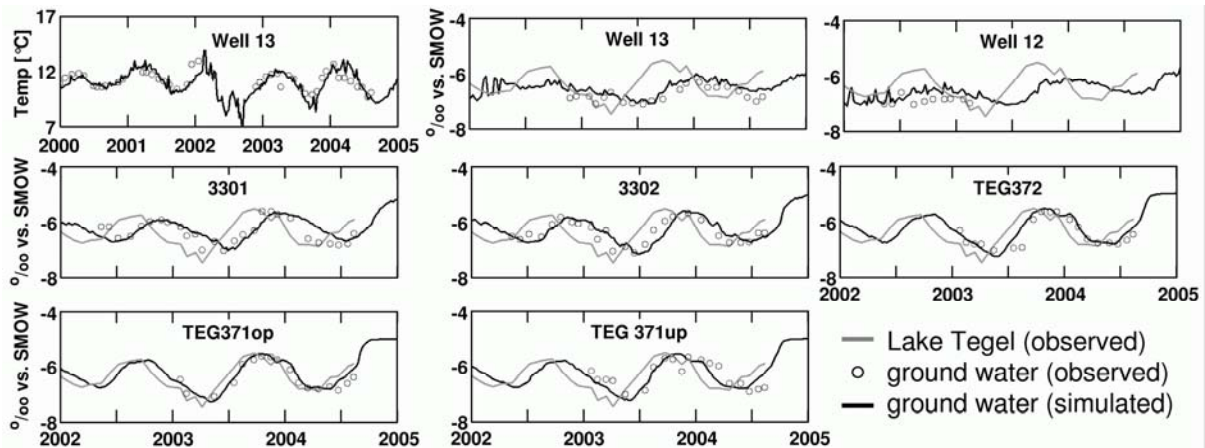


Figure 7: Selected results of transport modeling. ^{18}O is presented for observation wells 3301, 3302, TEG371op, TEG371up, TEG372, Well12 and Well13 for the period between 2002 and 2005. Temperature breakthrough is presented for Well13 for the period between 2000 and 2005.

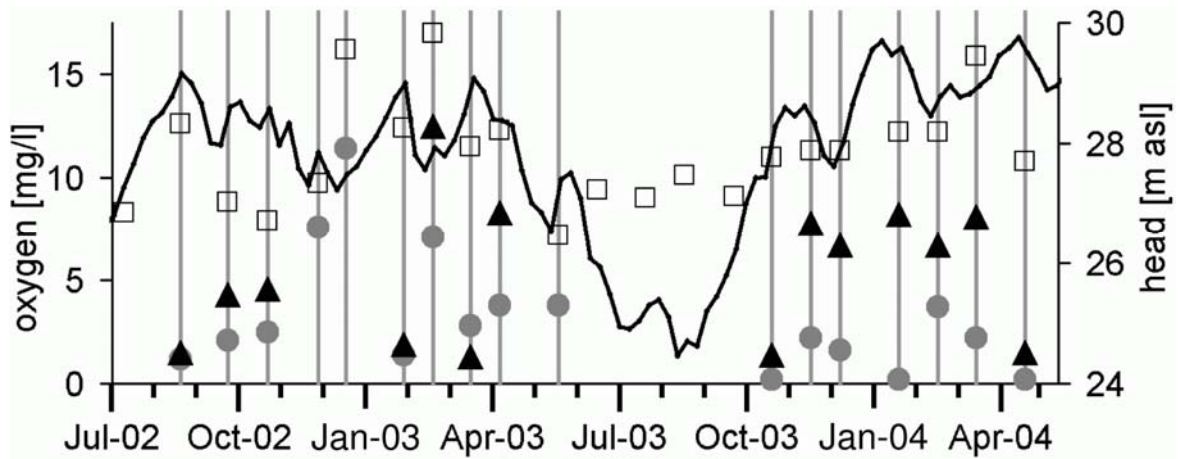


Figure 8: Oxygen concentrations in observation wells 3310 (triangles), 3311 (circles), and Lake Tegel (squares, all left axis). The simulated water table at 3311 is also shown (line, right axis).

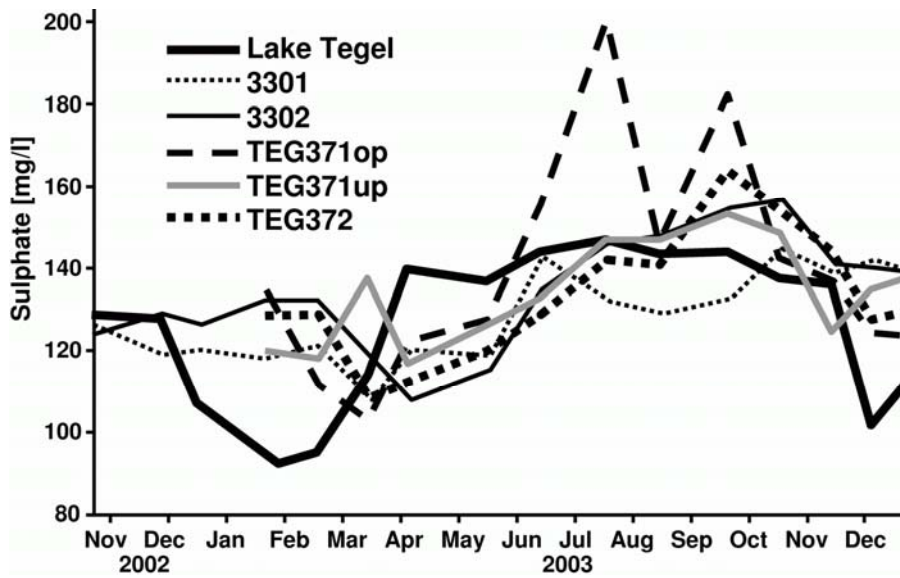


Figure 9: Observed sulphate concentrations in Lake Tegel and in observation wells. Observation wells 3302, TEG371op, TEG371up, and TEG372 show elevated concentrations around August 2003, observation well 3301 shows decreased concentrations in summer 2003.

parameters	Case 1	Case 2	Case 3	Case 4
space	8	8	8	2
time	-	2	45	-
unsaturated zone	-	-	-	2
leakance from third aquifer	1	1	1	1
total	9	11	54	5

Table 1: Parameterization of the different empirical leakance modeling concepts: the numerical values in the table denote the number of parameters used to calibrate the different approaches. The first three lines refer to leakance of the lake bed; the fourth line refers to inland conditions.

Φ at location	Case 1	Case 2	Case 3	Case 4
3301	75	47	46	50
TEG050	19	10	4	8
TEG051	11	7	1	8
TEG243*	55	43	13	26
TEG339	4	2	2	4
TEG340	30	18	3	16
TEG341	20	12	3	14
TEG350	16	9	4	12
6034	8	5	3	5
6053*	92	48	37	16
entire model	183	110	66	116

Table 2: Values of the objective function Φ for each observation well and for the entire model. Observation wells designated with an asterisk are not included in the optimization. Therefore, they can be used to assess whether the simulated processes can be transferred to other regions and conditions. The sum of each column, excluding the observation wells marked with an asterisk, is denoted by “entire model”.